

On numerically solving the complex eikonal equation using real ray-tracing methods: A comparison with the exact analytical solution

Václav Vavryčuk¹

ABSTRACT

The exact analytical solution of the complex eikonal equation describing P- and S-waves radiated by a point source situated in a simple type of isotropic viscoelastic medium was ascertained. The velocity-attenuation model is smoothly inhomogeneous with a constant gradient of the square of the complex slowness. The resultant traveltimes are complex; its real part describes the wave propagation and its imaginary part describes the attenuation effects. The solution was further used as a reference solution for numerical tests of the accuracy and robustness of two approximate ray-tracing approaches solving the complex eikonal equation: real elastic ray tracing and real viscoelastic ray tracing. Numerical modeling revealed that the real viscoelastic ray tracing method is unequivocally preferable to elastic ray tracing. It is more accurate and works even in situations when the elastic ray tracing fails. Also, the ray fields calculated by the real viscoelastic ray tracing are excellently reproduced even in the case when the elastic ray tracing yields completely distorted results. Compared with complex ray tracing, which is limited to simple types of media, the real viscoelastic ray tracing offers a fast and computationally straightforward procedure for calculating complex traveltimes in complicated 3D inhomogeneous attenuating structures.

INTRODUCTION

High-frequency asymptotic methods are frequently used in geophysics for modeling of waves propagating in complex geological structures because they are reasonably accurate and require almost no computer time compared with other numerical methods such as finite-difference or finite-element methods for calculating full waveforms. The high-frequency methods are based on solving

the eikonal equation for traveltimes, which is a fundamental equation extensively used in many seismic applications including travel-time tomography.

The eikonal equation can be solved using many different approaches (Nowack, 1992). It can be solved analytically in very simple models (Červený, 2001), but usually it is solved numerically. The most commonly used methods are finite-difference eikonal solvers (Vidale, 1988, 1990; Eaton, 1993), the fast marching method (Sethian, 1999; Sethian and Popovici, 1999; Yatziv et al., 2006), the network shortest-path method (Moser, 1991; Cheng and House, 1996), the wavefront construction method (Vinje et al., 1993), or finite-element methods (Giladi and Keller, 2001; Li et al., 2008). A classic and frequently applied approach is to solve the eikonal equation using Hamilton-Jacobi equations (Courant and Hilbert, 1989). This approach leads to solving a system of ordinary differential equations of the first order, called the “ray-tracing” equations. The ray-tracing solvers have been developed and widely applied to isotropic as well as anisotropic elastic media (Červený, 2001; Qian and Symes, 2001; Vavryčuk, 2001, 2003; Bulant and Klimeš, 2002).

The applicability of ray-tracing solvers also has been extended to media with attenuation. The attenuation is incorporated by replacing real-valued elastic parameters with complex-valued and frequency-dependent viscoelastic parameters (Auld, 1973; Carcione, 1990, 2007; Caviglia and Morro, 1992). Consequently, the eikonal equation and the ray-tracing equations become complex (Zhu and Chun, 1994; Chapman et al., 1999; Hanyga and Sereďyňska, 1999, 2000; Kravtsov et al., 1999; Kravtsov, 2005; Amodei et al., 2006). However, the complex ray tracing involves complications. It is more computationally demanding than real ray tracing, because rays become curves in complex space. Also, construction of the complex model in complex space brings difficulties, because the propagation velocity and attenuation are measured in real space but they have to be defined in the whole complex space. For simple velocity-attenuation models, the extension of the model parameters into complex space can be obtained in a formal mathematical way by analytic continuation. For example, complex ray tracing can be

Manuscript received by the Editor 27 October 2011; revised manuscript received 2 April 2012; published online 19 June 2012; corrected version published online 13 July 2012.

¹Institute of Geophysics, Academy of Sciences, Praha, Czech Republic. E-mail: vv@ig.cas.cz.
© 2012 Society of Exploration Geophysicists. All rights reserved.

performed readily for a homogeneous medium or for two homogeneous half-spaces with a planar interface (Vavryčuk, 2010). However, this approach fails for realistic 3D velocity models with interfaces, which cannot be analytically continued. Therefore, several alternative approaches have been proposed for solving the complex eikonal equation, based on real ray tracing (Gajewski and Pšenčík, 1992; Vavryčuk, 2008a, 2008b; Klimeš and Klimeš, 2011). These approaches are less accurate, but applicable to more realistic models.

In this paper, I present an analytical solution of the complex eikonal equation for P- and S-waves radiated by a point source situated in a simple type of isotropic viscoelastic medium. The model is smoothly inhomogeneous with a constant gradient of c^{-2} . The resultant traveltimes are complex; its real part describes the wave propagation and its imaginary part describes the attenuation effects. The solution is further used as a reference solution for numerical tests of the accuracy of solving the complex eikonal equation using two real ray-tracing approaches: real elastic ray tracing and real viscoelastic ray tracing. The real elastic ray tracing method (Gajewski and Pšenčík, 1992) is simple and straightforward, being applicable to weakly attenuating media. The rays are calculated in an elastic reference medium using the standard elastic ray theory, and attenuation effects are incorporated using perturbation formulas. A real viscoelastic ray-tracing technique was proposed recently by Vavryčuk (2008a). The rays are traced in a viscoelastic medium, but they are forced to lie in real space. In numerical tests, the accuracy of the elastic and viscoelastic ray-tracing methods is compared and the efficiency of both approaches is discussed.

COMPLEX EIKONAL EQUATION

The equation of motion in viscoelastic media reads

$$\rho\omega^2 u_i + (c_{ijkl} u_{k,l})_{,j} = 0, \quad (1)$$

where a comma represents differentiation, ρ is the real-valued density of the medium, ω is the real-valued circular frequency, $\mathbf{u} = \mathbf{u}(\mathbf{x}, \omega)$ is the complex-valued displacement, \mathbf{x} is the real-valued position vector, and $c_{ijkl} = c_{ijkl}(\mathbf{x}, \omega)$ are the complex-valued and frequency-dependent stiffness parameters, defined in isotropic media as

$$c_{ijkl} = \lambda\delta_{ij}\delta_{kl} + \mu(\delta_{ik}\delta_{jl} + \delta_{il}\delta_{jk}). \quad (2)$$

Parameters λ and μ are the Lamé coefficients. The real parts, λ^R and μ^R , describe elastic properties of the medium, while the imaginary parts, λ^I and μ^I , describe attenuation. The velocities for P- and S-waves,

$$c_P = \sqrt{\frac{\lambda + 2\mu}{\rho}}, \quad c_S = \sqrt{\frac{\mu}{\rho}}, \quad (3)$$

are complex-valued and frequency-dependent. The strength of attenuation is evaluated using the quality factor Q (Carcione, 2007, his equation 2.120),

$$Q_P = -\frac{\lambda^R + 2\mu^R}{\lambda^I + 2\mu^I}, \quad Q_S = -\frac{\mu^R}{\mu^I}. \quad (4)$$

The sign in equation 4 depends on the definition of the Fourier transform used for calculating the viscoelastic parameters in the frequency domain. When using the Fourier transform with the exponential term $\exp(-i\omega t)$, the minus signs in equation 4 must be omitted (see Vavryčuk, 2010).

If we assume a high-frequency signal $\mathbf{u} = \mathbf{u}(\mathbf{x}, \omega)$ described by complex-valued amplitude $\mathbf{U} = \mathbf{U}(\mathbf{x})$ and complex-valued travel-time $\tau = \tau(\mathbf{x})$,

$$u_i(\mathbf{x}, \omega) \cong U_i(\mathbf{x}) \exp[i\omega\tau(\mathbf{x})], \quad (5)$$

which propagates in the viscoelastic isotropic medium, we obtain that the traveltime must satisfy the eikonal equation,

$$c^2 p_i p_i = 1, \quad (6)$$

where c stands for the P- or S-wave velocity defined in equation 3, and \mathbf{p} is the complex-valued slowness vector

$$p_i = \frac{\partial\tau}{\partial x_i}. \quad (7)$$

The slowness vector \mathbf{p} can be decomposed into its real and imaginary parts,

$$p_i^R = \frac{\partial\tau^R}{\partial x_i}, \quad p_i^I = \frac{\partial\tau^I}{\partial x_i}, \quad (8)$$

which define the directions of the signal propagation and of the exponential amplitude decay, respectively. The eikonal equation can be rewritten in the following form (Červený, 2001)

$$H(\mathbf{x}, \mathbf{p}) = \frac{1}{2}(c^2 p_i p_i - 1) = 0, \quad (9)$$

where $H = H(\mathbf{x}, \mathbf{p})$ is the Hamiltonian, and vectors \mathbf{x} and \mathbf{p} are the canonical coordinates. Note that the Hamiltonian can be defined using the eikonal equation in other ways; see Červený (2001).

RAY-TRACING METHODS

Complex ray tracing

The complex eikonal equation 9 can be solved by applying the method of characteristics using the complex Hamilton-Jacobi equations (Kravtsov, 2005)

$$\frac{dx_i}{d\sigma} = \frac{\partial H}{\partial p_i}, \quad \frac{dp_i}{d\sigma} = -\frac{\partial H}{\partial x_i}, \quad \frac{d\tau}{d\sigma} = p_i \frac{\partial H}{\partial p_i}, \quad (10)$$

where σ is a complex-valued parameter along a ray. For $\sigma = \tau$ and H expressed in equation 9, the Hamilton-Jacobi equations yield the following system of complex ray-tracing equations

$$\frac{dx_i}{d\tau} = c^2 p_i, \quad \frac{dp_i}{d\tau} = -\frac{1}{c} \frac{\partial c}{\partial x_i}. \quad (11)$$

Having calculated the complex solution $\mathbf{x} = \mathbf{x}(\tau)$ from equations 11, we finally invert for complex travelttime τ as a function of real space coordinates \mathbf{x}^R ,

$$\tau = \tau(\mathbf{x}^R). \quad (12)$$

Equation 11 is formally identical with the real ray-tracing equation in elastic media (Červený, 2001). In complex ray theory, however, all quantities in equation 11 are complex. These include the canonical coordinates $\mathbf{x} = \mathbf{x}^R + i\mathbf{x}^I$ and $\mathbf{p} = \mathbf{p}^R + i\mathbf{p}^I$, which form a 12D phase space. The rays are trajectories in complex space, and the solution of the ray-tracing equations is sought in the 12D \mathbf{x} - \mathbf{p} phase space. When solving the two-point ray-tracing problem, the source and the receiver are positioned in real space, but the ray connecting them is, generally, a curve in complex space.

Unfortunately, complex ray-tracing encounters difficulties. The main difficulty is in model building, because the model must be defined in complex space. The phase velocity c needed in equation 11 is measured in real space, $c = c(\mathbf{x}^R)$, but it must be analytically continued to complex space, $c = c(\mathbf{x})$. This can be done for homogeneous or simple smoothly inhomogeneous media. Complex ray tracing also can be performed for two homogeneous half-spaces with a planar interface (Vavryčuk, 2010). However, the analytic continuation is difficult for realistic 3D inhomogeneous structures with curved interfaces. This restricts the applicability of complex ray theory. For some of the aspects of the analytic continuation, see Chapman et al. (1999).

In Appendix A, the analytical solution of the complex eikonal equation is presented for P- and S-waves radiated by a point source in a simple isotropic viscoelastic medium. The medium is inhomogeneous with a constant gradient of the square of the complex slowness c^{-2} . The complex solution is obtained from the real solution by analytic continuation. The rays are trajectories in complex space, while the source and the receiver lie in real space. The solution is exact and can serve as the reference solution for determining the accuracy of any approximate method.

The analytical solution of the complex eikonal equation also can be found for waves propagating in some simple inhomogeneous anisotropic viscoelastic media. For example, the complex ray-tracing equations can be solved for an SH-wave propagating in a transversely isotropic medium or for a P-wave propagating in an elliptic transversely isotropic medium, provided that the transverse isotropy is factorized (i.e., all complex stiffness parameters have a common dependence on \mathbf{x} , see Červený, 2001, his equation 3.6.34) and characterized by a constant gradient of the square of slowness c^{-2} .

Real viscoelastic ray tracing

Vavryčuk (2008a) proposes a method of solving the complex eikonal equation 9 using a real ray-tracing method. In his approach, the Hamiltonian for viscoelastic media is modified to keep rays as trajectories in real space. The imaginary part of the slowness vector \mathbf{p}^I is not an independent variable in the Hamiltonian equations as it is in complex ray theory, but it is calculated from the condition of stationarity of the complex-valued slowness vector. This condition ensures that the complex velocity vector \mathbf{v} ,

$$v_i = \frac{dx_i}{d\tau} \quad (13)$$

is homogeneous, meaning that the real and imaginary parts of \mathbf{v} are parallel. Consequently, the ray direction is always real. The approach is also developed for anisotropic media. The stationary slowness vector is homogeneous in isotropic media, but inhomogeneous in anisotropic media, where real and imaginary parts of the slowness vector can form an arbitrary angle. In isotropic media, the ray-tracing equations read (Vavryčuk, 2008a)

$$\frac{dx_i}{d\tau^R} = V^2 p_i^R, \quad \frac{dp_i^R}{d\tau^R} = -\frac{1}{V} \frac{\partial V}{\partial x_i}, \quad \frac{d\tau^I}{d\tau^R} = -\frac{c^I}{c^R}, \quad (14)$$

where V is the real-valued ray velocity calculated from the complex-valued phase velocity c as,

$$V = \frac{1}{(c^{-1})^R}. \quad (15)$$

Equation 14 yields for τ^I :

$$\tau^I = -\int_{\tau_0^R}^{\tau^R} \frac{c^I}{c^R} d\tau^R. \quad (16)$$

Because the real viscoelastic ray-tracing method is an approximate approach, equations 14–16 yield results that are not fully self-consistent. For example, the ray field is constructed under the assumption of homogeneity of the complex velocity vector \mathbf{v} and of the complex slowness vector \mathbf{p} . However, if the imaginary part of the slowness vector \mathbf{p} is calculated as the gradient of τ^I obtained from equation 16,

$$p_i^I = \frac{\partial \tau^I}{\partial x_i}, \quad (17)$$

we can check that the resultant slowness vector, $\mathbf{p} = \mathbf{p}^R + \mathbf{p}^I$, where \mathbf{p}^R is calculated from equation 14, is no longer stationary. Hence, the condition of the stationary slowness vector is applied as an initial approximation when calculating \mathbf{x} and \mathbf{p}^R by equation 14. However, after constructing the real ray fields, it is more appropriate to apply equation 17 to obtain a more correct value for \mathbf{p}^I . In this way, the exact complex velocity vector \mathbf{v} and the complex slowness vector \mathbf{p} are better approximated, because they are inherently inhomogeneous.

Having calculated the complex travelttime τ using equations 14 and 16, we can define isochrones and gradient curves, called “rays.” The real and imaginary isochrones are formed by points of constant τ^R and τ^I , respectively. The propagation and attenuation rays are curves orthogonal to the real and imaginary isochrones (see Figure 1). If the propagation and attenuation curves coincide, the complex slowness vector \mathbf{p} is homogeneous. In most cases, however, the propagation and attenuation rays differ and vector \mathbf{p} is inhomogeneous. The real and imaginary isochrones, as well as the propagation and attenuation rays, are curves defined in real space; they provide a complete description of the kinematic and dynamic properties of wavefields. The propagation rays describe the trajectories along which energy is propagated and the travelttime is minimum (or stationary). The attenuation rays describe the trajectories along which the damping of energy of signals is maximum (or stationary). The propagation and attenuation rays can be constructed for exact as well as for approximate solutions of the

complex eikonal equation. For a point source situated in an attenuating medium with no elastic areas, the propagation and attenuation rays originate at the source (see Figure 1).

Because rays are forced to lie in real space, the method is approximate. On the other hand, the real ray theory is simple and applicable to a broad family of models of the medium, and its computational requirements are roughly the same as for ray tracing in elastic media.

Real elastic ray tracing

A simple method to incorporate attenuation into the standard real ray theory is to consider a viscoelastic medium as the perturbation of a perfectly elastic medium. The rays are traced in the elastic reference medium and the effects of attenuation are calculated by first-order perturbations (Červený, 2001, Section 5.5; Vavryčuk, 2008b). The ray-tracing equations are identical to those for the elastic reference medium, with the addition of an equation for τ^I

$$\frac{dx_i}{d\tau^R} = V_0^2 p_i^R, \quad \frac{dp_i^R}{d\tau^R} = -\frac{1}{V_0} \frac{\partial V_0}{\partial x_i}, \quad \frac{d\tau^I}{d\tau^R} = \frac{1}{2Q}. \quad (18)$$

Velocity V_0 is the real-valued reference velocity in the reference elastic medium,

$$V_0 = \sqrt{(c^2)^R}. \quad (19)$$

The imaginary traveltime τ^I is sometimes called the “global absorption coefficient” (Červený, 2001), being calculated from equations 18 by a quadrature along the reference ray

$$\tau^I = \frac{1}{2} \int_{\tau_0^R}^{\tau^R} \frac{d\tau^R}{Q}. \quad (20)$$

The imaginary part of the slowness vector \mathbf{p} is calculated as the gradient of τ^I .

This approach is approximate and performs best for weakly attenuating media. Its accuracy can be enhanced by incorporating higher-order perturbations. Similar to the real viscoelastic ray approach, the elastic ray approach is applicable to a broad family of medium models, and the computational requirements are comparable with those of ray tracing in elastic media.

When comparing equations 14 and 18, we find that the elastic and viscoelastic ray approaches are similar. Both approaches solve for \mathbf{x} , \mathbf{p}^R and τ^I as a function of τ^R and produce real rays. However, the computed ray fields and traveltimes $\tau = \tau(\mathbf{x})$ are not identical. The differences are caused by a different definition of the real-valued velocity and by a different formula for calculating τ^I . The differences originate from different assumptions and approximations used in both approaches and are more pronounced in media with strong attenuation. In media with weak attenuation, they are of the order of the second and higher perturbations. For example, if we take into account that the imaginary part of the complex velocity c^I is much smaller than its real part c^R under weak attenuation, $c^I \ll c^R$, we obtain

$$\begin{aligned} \frac{1}{2Q} &= -\frac{1}{2} \frac{(c^2)^I}{(c^2)^R} = -\frac{1}{2} \frac{(c^R c^R + 2ic^R c^I - c^I c^I)^I}{(c^R c^R + 2ic^R c^I - c^I c^I)^R} \\ &\cong -\frac{1}{2} \frac{2c^R c^I}{c^R c^R} = -\frac{c^I}{c^R}, \end{aligned} \quad (21)$$

and equation 20 transforms into equation 16.

NUMERICAL MODELING

In this section, the accuracy of the ray-tracing methods is examined numerically. Two models of a viscoelastic medium, model A and model B, are considered. The models are smoothly inhomogeneous, with a constant gradient of c^{-2} . For such models, an exact solution of the complex eikonal equation can be found analytically by using complex ray tracing (see Appendix A). The complex phase velocity c reads

$$c^{-2}(\mathbf{x}) = c_0^{-2} + A_i x_i, \quad (22)$$

where $c_0 = 1$ km/s, $A_1 = 0.1i$, $A_2 = 0$ and $A_3 = 0$ for model A, and $c_0 = 1$ km/s, $A_1 = 0.1i$, $A_2 = 0$ and $A_3 = -0.15$ for model B. The phase velocity c_0 is in km/s, the gradients A_i are in s^2/km^3 . The eikonal equation is solved in the x - z plane. The waves are excited by a point source situated at the origin of coordinates.

The models A and B are artificial. The gradients of complex velocity c are very strong and behave independently for the real and imaginary parts of c . In both models, the gradient in attenuation (gradient in c^I) is along the x -axis. The Q -factor decreases from the value of $Q = \infty$ at $x = 0$ to the value of $Q = 1$ at $x = 10$ km. Model B also displays a real vertical gradient in c^{-2} . In real materials, the attenuation and the real velocity gradients are not so strong and they are usually correlated. High-velocity structures are associated with low attenuation and vice versa. Here, the models are

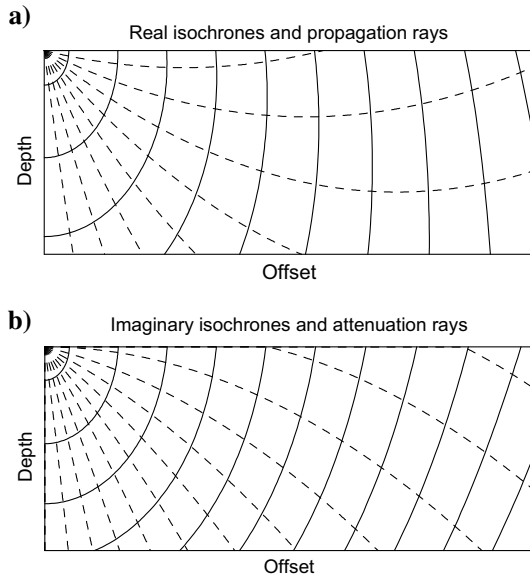


Figure 1. Schematic plots of (a) real isochrones and propagation rays and of (b) imaginary isochrones and attenuation rays for a point source situated at an attenuating isotropic medium. The solid lines show the isochrones, the dashed lines show the rays. The propagation and attenuation ray fields are, in general, different, and the corresponding complex slowness vector is inhomogeneous.

used just as extremes for checking the robustness of the real ray-tracing methods. The methods will provide more accurate results when applied to realistic models where attenuation is usually not so strong.

Figures 2 and 3 display velocity models A and B, respectively. Plots (a) and (b) show the real and imaginary parts of the square of the complex slowness c^{-2} , plots (c) and (d) show the real and imaginary parts of the complex phase velocity c . Model A is simpler

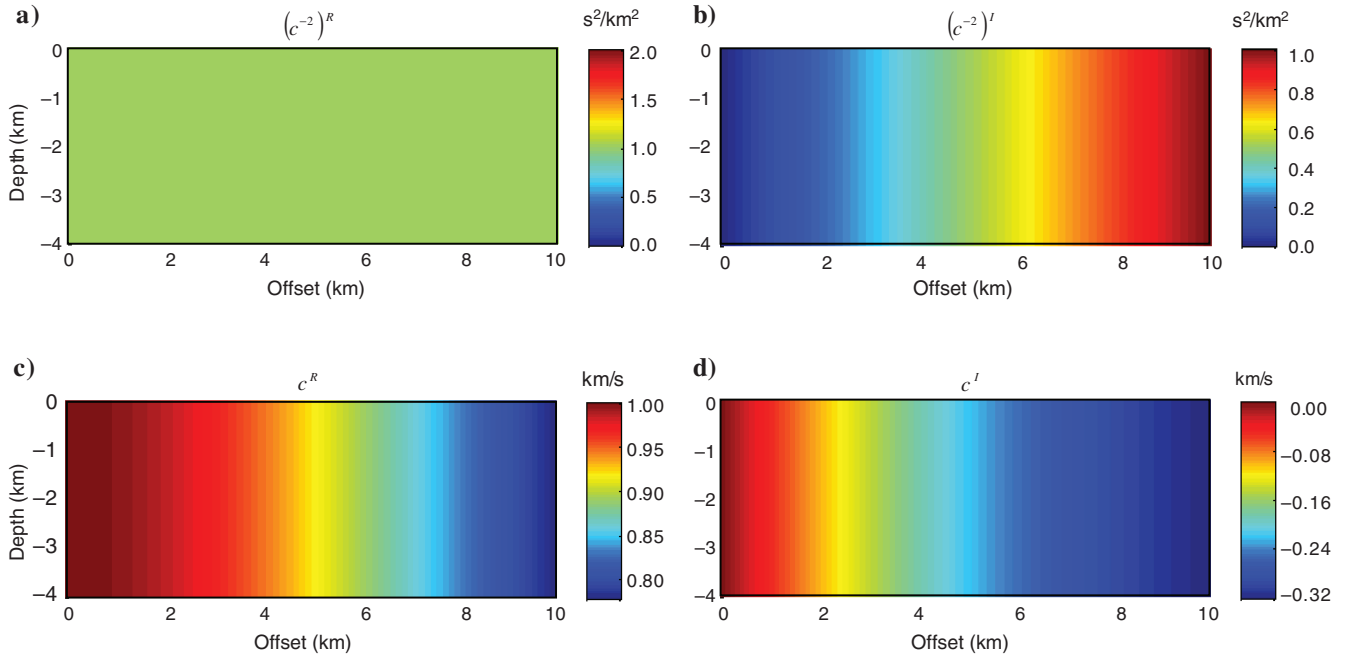


Figure 2. (a) Real and (b) imaginary parts of the square of slowness c^{-2} , and (c) real and (d) imaginary parts of complex phase velocity c in model A. The color scales in (a) and (b) are in s^2/km^2 , the color scales in (c) and (d) are in km/s .

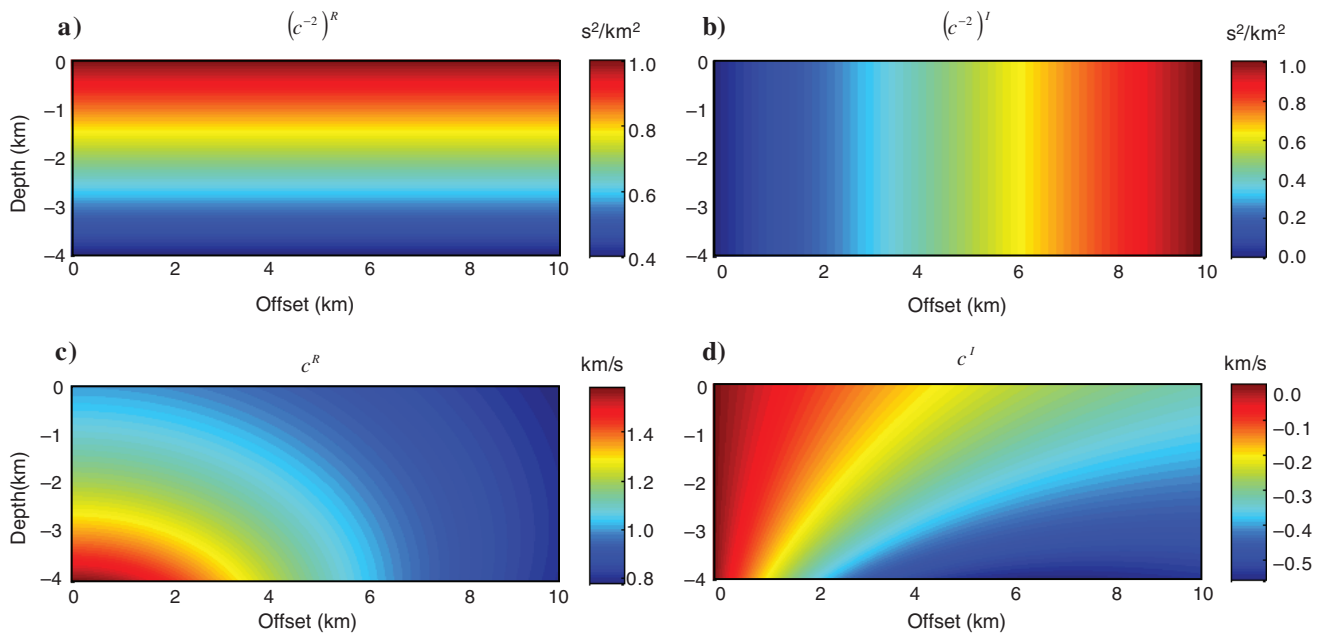


Figure 3. (a) Real and (b) imaginary parts of the square of slowness c^{-2} , and (c) real and (d) imaginary parts of complex phase velocity c in model B. The color scales in (a) and (b) are in s^2/km^2 , the color scales in (c) and (d) are in km/s .

than model B because it is characterized only by horizontal gradients in c^R and c^I . In model B, the real vertical gradient in c^{-2} and the imaginary horizontal gradient in c^{-2} superimpose and produce a complicated pattern in $c^R = c^R(x, z)$ and $c^I = c^I(x, z)$.

Figure 4 shows the solutions of the complex eikonal equation using complex ray tracing, real viscoelastic ray tracing, and real

elastic ray tracing in model A. To densely cover the region under study, the rays were shot from the source at $\mathbf{x}_S = (0, 0)^T$ with take-off angles ranging from 0° to 90° , with a step of 0.25° . The maximum distance between two consecutive points along a ray was 0.02 km. Plots 4a and 4b show the exact complex traveltime calculated using complex ray tracing. Plots 4c and 4d show the errors of the elastic ray tracing and plots 4e and 4f show the errors of the viscoelastic ray tracing. The errors are calculated at each point of the model as the difference between the exact and approximate solution and evaluated in percent. The maximum errors of the complex traveltime calculated by the viscoelastic ray tracing attain values up to 0.15%. The elastic ray tracing yields errors remarkably higher; up to 6% in τ^R , and up to 30% in τ^I .

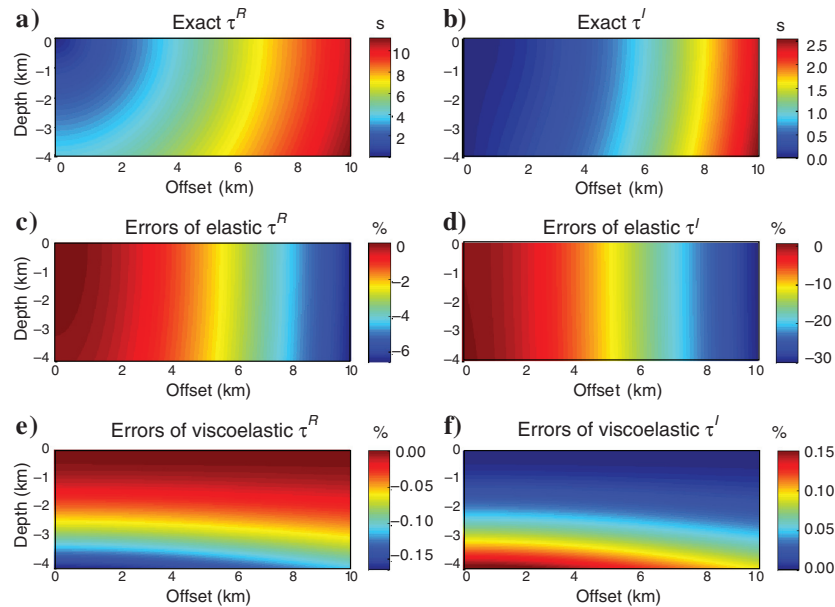


Figure 4. Complex traveltime and its errors in model A: (a) real part of the exact traveltime, τ^R ; (b) imaginary part of the exact traveltime, τ^I ; (c) errors of τ^R produced by the elastic ray tracing; (d) errors of τ^I produced by the elastic ray tracing; (e) errors of τ^R produced by the viscoelastic ray tracing; (f) errors of τ^I produced by the viscoelastic ray tracing. The traveltime (a and b) is in seconds, the errors of the traveltime (c-f) are in percentages.

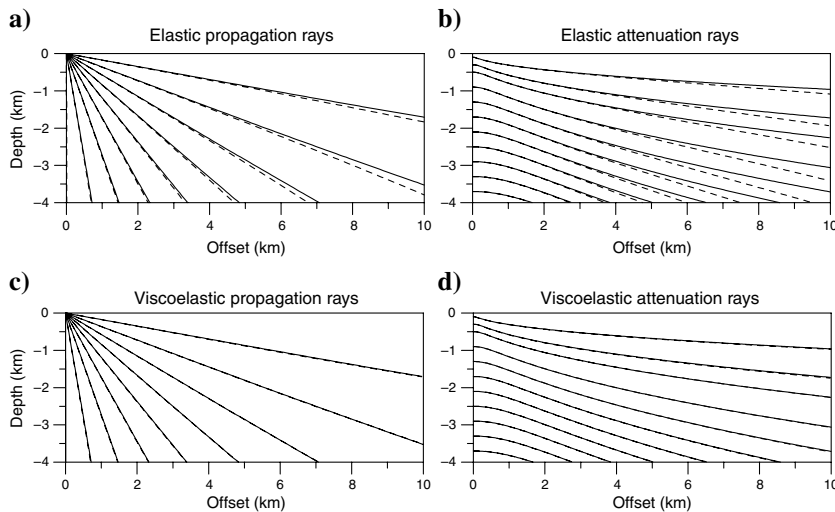


Figure 5. Ray fields in model A. Solid line — exact solution calculated using the complex ray tracing; dashed line — approximate solution calculated (a and b) using the elastic ray tracing, and (c and d) using the viscoelastic ray tracing. Left-hand plots show the propagation rays, right-hand plots show the attenuation rays. The propagation rays are shot at the origin of coordinates in incidences from 10° to 90° with a step of 10° . The attenuation rays are shot at $x = 0$ and $z = -0.1, -0.3, -0.5, -0.9, -1.3, -1.7, -2.1, -2.5, -2.9, -3.3,$ and -3.7 km.

The errors in τ influence the ray fields calculated from gradients of τ . Figure 5 shows the propagation (left-hand plots) and attenuation (right-hand plots) rays in model A. The rays were calculated as curves of the steepest ascent of the real and imaginary parts of the complex traveltime τ . The traveltime gradients were computed numerically using finite differences. Because traveltime τ was calculated on a very dense grid of points in the studied region, the errors introduced by approximating the gradients by finite differences are negligible, i.e., at least of two orders smaller than the errors originating from real ray-tracing approximations. As expected, the propagation rays start at the point source situated at the origin of coordinates. The rays are approximately straight lines. However, the attenuation rays behave differently. The attenuation rays do not originate at the source as shown in Figure 1, but on the vertical axis below the source. Because the model is not attenuating everywhere, but is elastic at $x = 0$, the imaginary traveltime τ^I is zero along the whole left vertical border of the region under study. Consequently, the attenuation rays have a starting direction perpendicular to this border. The ray direction changes with increasing traveltime and the attenuation rays form a family of smooth quasi-parallel curves. With increasing traveltime, approximate rays calculated by elastic ray tracing begin to deviate from the exact rays. The differences are visible in propagation as well as in attenuation ray fields. The errors in the attenuation ray fields are slightly larger. In contrast, viscoelastic ray tracing predicts ray fields identical to the exact ones. We emphasize that because remarkable differences between propagation and attenuation ray fields are observed, the real and imaginary parts of the complex slowness vector have different directions and the complex slowness vector is inhomogeneous.

Figures 6 and 7 are analogous to Figures 4 and 5, except for model B. Because model B is more

complicated than model A, the approximate methods provide a lower accuracy result. Figure 6 indicates that elastic ray tracing yields errors in τ^R up to 15% and errors in τ^I up to 60%. Hence, wave attenuation is reproduced with considerably lower accuracy than

the wave propagation. The viscoelastic ray tracing yields errors in τ^R up to 1% and in τ^I up to 2%. The geometry of the propagation rays is distinctly distorted in the case of the elastic ray tracing, and completely fails for the attenuation rays (see Figure 7). On the other hand, viscoelastic ray tracing predicts ray fields almost identical to the exact ones.

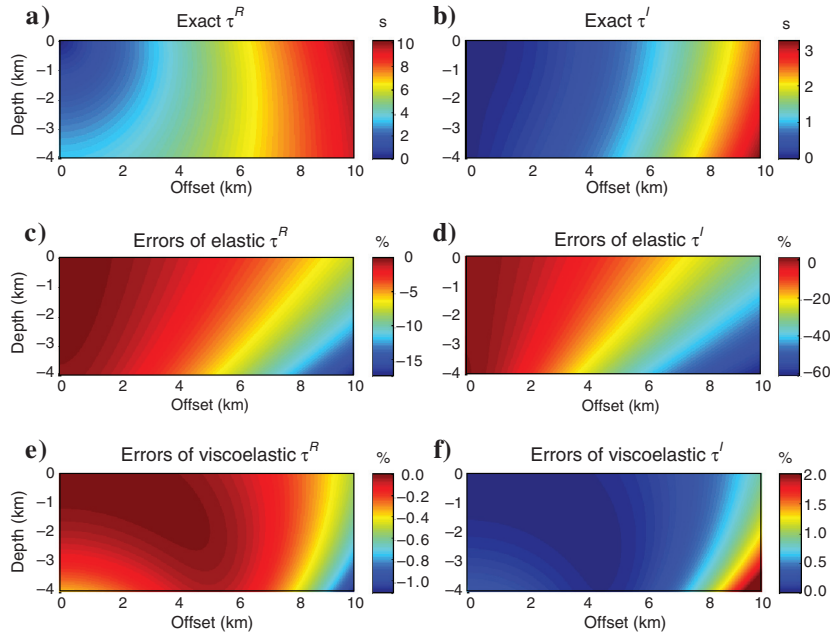


Figure 6. Complex traveltimes and its errors in model B: (a) real part of the exact traveltimes, τ^R ; (b) imaginary part of the exact traveltimes, τ^I ; (c) errors of τ^R produced by the elastic ray tracing; (d) errors of τ^I produced by the elastic ray tracing; (e) errors of τ^R produced by the viscoelastic ray tracing; (f) errors of τ^I produced by the viscoelastic ray tracing. The traveltimes (a and b) is in seconds, the errors of the traveltimes (c-f) are in percentages.

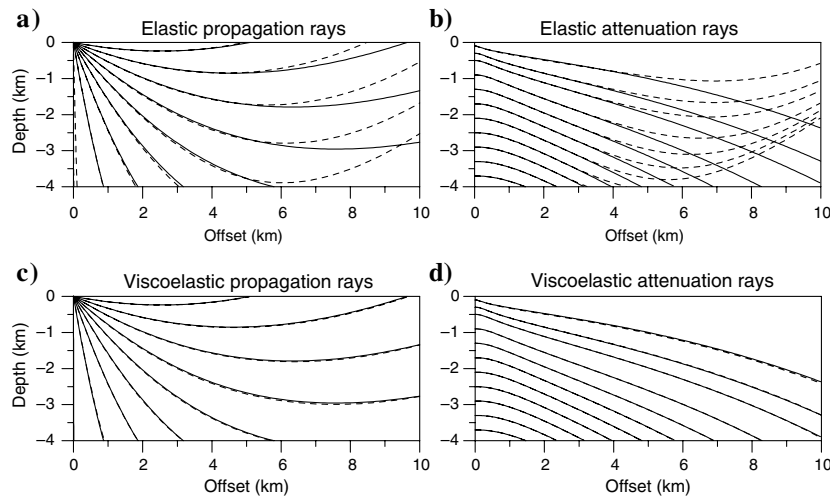


Figure 7. Ray fields in model B. Solid line — exact solution calculated using the complex ray tracing, dashed line — approximate solution calculated (a and b) using the elastic ray tracing, and (c and d) using the viscoelastic ray tracing. Left-hand plots show the propagation rays, right-hand plots show the attenuation rays. The propagation rays are shot at the origin of coordinates in incidences from 10° to 90° with a step of 10° . The attenuation rays are shot at $x = 0$ and $z = -0.1, -0.3, -0.5, -0.9, -1.3, -1.7, -2.1, -2.5, -2.9, -3.3,$ and -3.7 km.

CONCLUSIONS

This paper presents one particular analytical solution of the complex eikonal equation. The solution physically describes traveltimes, rays, and attenuation of P- and S-waves generated by a point source in an isotropic medium with a constant gradient of c^{-2} . The solution can also be generalized for an SH-wave propagating in a factorized transversely isotropic medium, or for a P-wave propagating in a factorized elliptically transversely isotropic medium. The analytical solution is a useful tool for testing the accuracy of various approximate wave propagation approaches developed for attenuating media.

The complex analytical solution is used for accuracy tests of two approximate real ray approaches, which offer a fast and computationally straightforward calculation of complex traveltimes in 3D inhomogeneous attenuating structures. Although the computational demands of the both approaches are the same, the tests indicate that real viscoelastic ray tracing is more efficient and more accurate. The procedure works even for large velocity gradients and for strong attenuation. It yields accurate results in models in which real elastic ray tracing might fail. Because the viscoelastic ray-tracing method performs better with no additional costs in computational time or in programming, it is definitely preferable to real elastic ray tracing.

The computational scheme of the real viscoelastic ray tracing algorithm in isotropic viscoelastic media is very similar to that in isotropic elastic media. Hence, existing computer codes working in purely elastic media can be simply generalized to attenuating media. In models with the Q -factor independent of frequency, the computational demands on the ray tracing are, in principle, the same as in the elastic case. In models with frequency-dependent Q , the ray-tracing procedure must be run repeatedly at different frequencies. The real viscoelastic ray tracing method is also applicable to anisotropic viscoelastic media, but the procedure is computationally more demanding.

ACKNOWLEDGMENTS

I thank Luděk Klimeš, Jeff Shragge, and four anonymous reviewers for their comments. The work was supported by the Grant Agency of the Academy of Sciences of the Czech Republic, Grant No. IAA300120801.

APPENDIX A

ANALYTICAL COMPLEX RAY TRACING IN A MEDIUM WITH A CONSTANT GRADIENT OF C^{-2}

Similarly as for the real ray tracing in elastic media (see Červený, 2001, Sec. 3.4), the simplest analytical solution of the complex ray tracing is obtained for a medium with a constant gradient of the square of slowness c^{-2} . Let us assume that c^{-2} is given by

$$c^{-2}(\mathbf{x}) = c_0^{-2} + A_i x_i, \quad (\text{A-1})$$

and consider only that part of the space where $(c^{-2})^R > 0$. All quantities in equation A-1 are generally complex. The ray-tracing equation 11 yields the following solution

$$x_i(\sigma) = x_{i0} + p_{i0}(\sigma - \sigma_0) + \frac{1}{4}A_i(\sigma - \sigma_0)^2, \quad (\text{A-2})$$

$$p_i(\sigma) = p_{i0} + \frac{1}{2}A_i(\sigma - \sigma_0), \quad (\text{A-3})$$

$$\begin{aligned} \tau(\sigma) = \tau_0 + c_0^{-2}(\sigma - \sigma_0) + \frac{1}{2}A_i p_{i0}(\sigma - \sigma_0)^2 \\ + \frac{1}{12}A_i A_i (\sigma - \sigma_0)^3, \end{aligned} \quad (\text{A-4})$$

where σ is the complex parameter along the ray. Let us assume the point source is at the center of the coordinates and parameter σ is zero at the source

$$\mathbf{x}_0 = (0, 0, 0)^T, \quad \sigma_0 = 0. \quad (\text{A-5})$$

The receiver lies in real space, with coordinates $\mathbf{x}^R = (x_1^R, x_2^R, x_3^R)^T$. Equation A-2, together with the eikonal equation at the source,

$$p_{i0} p_{i0} = c_0^{-2}, \quad (\text{A-6})$$

represents a system of four complex equations for four complex unknowns: p_{10} , p_{20} , p_{30} , and σ . Eliminating slowness components p_{10} , p_{20} , and p_{30} , we obtain a quadratic equation for σ^2 ,

$$\frac{1}{16}A_i A_i \sigma^4 - \left(p_0^2 + \frac{1}{2}A_i x_i^R \right) \sigma^2 + x_i^R x_i^R = 0. \quad (\text{A-7})$$

Solving this equation for σ , we can evaluate the slowness vector \mathbf{p}_0 at the source \mathbf{x}_0 , slowness vector $\mathbf{p}(\mathbf{x}^R)$ at the receiver \mathbf{x}^R , and traveltimes at the receiver $\tau(\mathbf{x}^R)$ from equations A-2, A-3, and A-4.

REFERENCES

Amodei, D., H. Keers, W. Vasco, and L. Johnson, 2006, Computation of uniform wave forms using complex rays: *Physical Review E*, **73**, 036704, 1–14, doi: [10.1103/PhysRevE.73.036704](https://doi.org/10.1103/PhysRevE.73.036704).
 Auld, B. A., 1973, *Acoustic fields and waves in solids*: Wiley.
 Bulant, P., and L. Klimeš, 2002, Numerical algorithm of the coupling ray theory in weakly anisotropic media: *Pure and Applied Geophysics*, **159**, 1419–1435, doi: [10.1007/s00024-002-8690-2](https://doi.org/10.1007/s00024-002-8690-2).
 Carcione, J. M., 1990, Wave propagation in anisotropic linear viscoelastic media: Theory and simulated wavefields: *Geophysical Journal International*, **101**, 739–750. Erratum: 111 (1992) 191, doi: [10.1111/gji.1990.101.issue-3](https://doi.org/10.1111/gji.1990.101.issue-3).

Carcione, J. M., 2007, *Wave fields in real media: Theory and numerical simulation of wave propagation in anisotropic, anelastic, porous and electromagnetic media*: Elsevier.
 Caviglia, G., and A. Morro, 1992, *Inhomogeneous waves in solids and fluids*: World Scientific.
 Červený, V., 2001, *Seismic ray theory*: Cambridge University Press.
 Chapman, S. J., J. M. H. Lawry, J. R. Ockendon, and R. H. Tew, 1999, On the theory of complex rays: *SIAM Review*, **41**, 417–509, doi: [10.1137/S0036144599352058](https://doi.org/10.1137/S0036144599352058).
 Cheng, N., and L. House, 1996, Minimum traveltimes calculation in 3D graph theory: *Geophysics*, **61**, 1895–1898, doi: [10.1190/1.1444104](https://doi.org/10.1190/1.1444104).
 Courant, R., and D. Hilbert, 1989, *Methods of mathematical physics I, II*: Wiley & Sons.
 Eaton, D. W. S., 1993, Finite difference traveltimes calculation for anisotropic media: *Geophysical Journal International*, **114**, 273–280, doi: [10.1111/gji.1993.114.issue-2](https://doi.org/10.1111/gji.1993.114.issue-2).
 Gajewski, D., and I. Pšenčík, 1992, Vector wavefield for weakly attenuating anisotropic media by the ray method: *Geophysics*, **57**, 27–38, doi: [10.1190/1.1443186](https://doi.org/10.1190/1.1443186).
 Giladi, E., and J. B. Keller, 2001, A hybrid numerical asymptotic method for scattering problems: *Journal of Computational Physics*, **174**, 226–247, doi: [10.1006/jcph.2001.6903](https://doi.org/10.1006/jcph.2001.6903).
 Hanyga, A., and M. Seredyńska, 1999, Asymptotic ray theory in poro- and viscoelastic media: *Wave Motion*, **30**, 175–195, doi: [10.1016/S0165-2125\(98\)00053-5](https://doi.org/10.1016/S0165-2125(98)00053-5).
 Hanyga, A., and M. Seredyńska, 2000, Ray tracing in elastic and viscoelastic media: *Pure and Applied Geophysics*, **157**, 679–717, doi: [10.1007/PL00001114](https://doi.org/10.1007/PL00001114).
 Klimeš, M., and L. Klimeš, 2011, Perturbation expansion of complex-valued traveltimes along real-valued reference rays: *Geophysical Journal International*, **186**, 751–759, doi: [10.1111/j.1365-246X.2011.05054.x](https://doi.org/10.1111/j.1365-246X.2011.05054.x).
 Kravtsov, Yu. A., 2005, *Geometrical optics in engineering physics*: Alpha Science.
 Kravtsov, Yu. A., G. W. Forbes, and A. A. Asatryan, 1999, Theory and applications of complex rays, in E. Wolf, ed.: *Progress in optics*, **39**, 3–62.
 Li, F., Ch.-W. Shu, Y.-T. Zhang, and H. Zhao, 2008, A second order discontinuous Galerkin fast sweeping method for eikonal equations: *Journal of Computational Physics*, **227**, 8191–8208, doi: [10.1016/j.jcp.2008.05.018](https://doi.org/10.1016/j.jcp.2008.05.018).
 Moser, T. J., 1991, The shortest path calculation of seismic rays: *Geophysics*, **56**, 59–67, doi: [10.1190/1.1442958](https://doi.org/10.1190/1.1442958).
 Nowack, R. L., 1992, Wavefronts and solutions of the eikonal equation: *Geophysical Journal International*, **110**, 55–62, doi: [10.1111/gji.1992.110.issue-1](https://doi.org/10.1111/gji.1992.110.issue-1).
 Qian, J., and W. W. Symes, 2001, Paraxial eikonal solvers for anisotropic quasi-P travel times source: *Journal of Computational Physics*, **173**, 256–278, doi: [10.1006/jcph.2001.6875](https://doi.org/10.1006/jcph.2001.6875).
 Sethian, J. A., 1999, Fast marching methods: *SIAM Review*, **41**, 199–235, doi: [10.1137/S0036144598347059](https://doi.org/10.1137/S0036144598347059).
 Sethian, J. A., and A. M. Popovici, 1999, 3D traveltimes computation using the fast marching method: *Geophysics*, **64**, 516–523, doi: [10.1190/1.1444558](https://doi.org/10.1190/1.1444558).
 Vavryčuk, V., 2001, Ray tracing in anisotropic media with singularities: *Geophysical Journal International*, **145**, 265–276, doi: [10.1046/j.0956-540x.2001.01387.x](https://doi.org/10.1046/j.0956-540x.2001.01387.x).
 Vavryčuk, V., 2003, Behavior of rays near singularities in anisotropic media: *Physical Review B*, **67**, 054105, doi: [10.1103/PhysRevB.67.054105](https://doi.org/10.1103/PhysRevB.67.054105).
 Vavryčuk, V., 2007, Ray velocity and ray attenuation in homogeneous anisotropic viscoelastic media: *Geophysics*, **72**, no. 6, D119–D127, doi: [10.1190/1.2768402](https://doi.org/10.1190/1.2768402).
 Vavryčuk, V., 2008a, Real ray tracing in anisotropic viscoelastic media: *Geophysical Journal International*, **175**, 617–626, doi: [10.1111/gji.2008.175.issue-2](https://doi.org/10.1111/gji.2008.175.issue-2).
 Vavryčuk, V., 2008b, Velocity, attenuation and quality factor in anisotropic viscoelastic media: A perturbation approach: *Geophysics*, **73**, no. 5, D63–D73, doi: [10.1190/1.2921778](https://doi.org/10.1190/1.2921778).
 Vavryčuk, V., 2010, Behaviour of rays at interfaces in anisotropic viscoelastic media: *Geophysical Journal International*, **181**, 1665–1677, doi: [10.1111/j.1365-246X.2010.04583.x](https://doi.org/10.1111/j.1365-246X.2010.04583.x).
 Vidale, J. E., 1988, Finite-difference traveltimes calculation: *Bulletin of the Seismological Society of America*, **78**, 2062–2076.
 Vidale, J. E., 1990, Finite-difference calculations of traveltimes in three dimensions: *Geophysics*, **55**, 521–526, doi: [10.1190/1.1442863](https://doi.org/10.1190/1.1442863).
 Vinje, V., E. Iversen, and H. Gjøystdal, 1993, Traveltimes and amplitude estimation using wavefront construction: *Geophysics*, **58**, 1157–1166, doi: [10.1190/1.1443499](https://doi.org/10.1190/1.1443499).
 Yatziv, L., A. Bartesaghi, and G. Sapiro, 2006, O(N) implementation of the fast marching algorithm: *Journal of Computational Physics*, **212**, 393–399, doi: [10.1016/j.jcp.2005.08.005](https://doi.org/10.1016/j.jcp.2005.08.005).
 Zhu, T. F., and K. Y. Chun, 1994, Complex rays in elastic and anelastic media: *Geophysical Journal International*, **119**, 269–276, doi: [10.1111/gji.1994.119.issue-1](https://doi.org/10.1111/gji.1994.119.issue-1).